



Supporting Information for ”CAICS: A glacial geomorphic marker for the study of debris-covered glaciers on Mars”

Léo Scordia¹, Susan J. Conway¹, Andreas Johnsson², Noé Le Becq¹, Cynthia Sassenroth², Jakob Heyman²

¹Nantes Université, Univ Angers, Le Mans Université, CNRS, Laboratoire de Planétologie et Géosciences, LPG UMR 6112, 44000

Nantes, France

²Department of Earth Sciences, University of Gothenburg, SE-405 30 Gothenburg, Sweden

Contents of this file

1. Text S1
2. Table S1
3. Figures S1 to S5

Additional Supporting Information (Files uploaded separately)

1. Dataset S1: CAICS-producing_Craters_Northern_Hemisphere_dataset_Scordia_2025.csv

Introduction This Supporting Information provides additional details on the dataset and figures related to Crater-Associated Irregular Cellular Structures (CAICS) on Mars. The

Corresponding author: L. Scordia, Nantes Université, Univ Angers, Le Mans Université, CNRS, Laboratoire de Planétologie et Géosciences, LPG UMR 6112, 44000 Nantes, France (e-mail addresses: leo.scordia@univ-nantes.fr / scordia.leo.sci@gmail.com)

supplementary figures illustrate morphological comparisons between CAICS and other landforms, as well as density maps of craters and glaciers. These data support the quantitative analyses and interpretations presented in the main text.

Data Set S1. CAICS-producing craters dataset. The full dataset of CAICS-producing craters is available as a CSV file (CAICS-producing_Craters_Northern_Hemisphere_dataset_Scordia_2025.csv).

Text S1. CAICS-producing Craters Dataset. A dataset of CAICS-producing craters identified in the northern hemisphere of Mars is provided as a comma-separated values (CSV) file entitled **CAICS-producing_Craters_Northern_Hemisphere_dataset_Scordia_2025.csv**. This dataset contains the full list of craters analyzed in this study and constitutes the basis for all quantitative analyses presented in the main text and supplementary figures.

Each row corresponds to an individual crater, and columns report crater location, morphometric properties, elevation measurements, and mobility metrics derived in this work. Where applicable, crater identifiers ("id_Rob_Hyn_CraterDatabase") from the global Mars crater database (Robbins & Hynek, 2012) are reported to enable cross-referencing with existing catalogs. Crater geographic coordinates are provided in latitude and longitude ("Crater_Longitude(deg)", "Crater_Latitude(deg)"), on a sphere with a radius of 3396190 m. Crater size parameters include diameter and radius ("Crater_Diameter(km)", "Crater_Radius(km)"), while elevation fields report outer crater slope mean elevation and the elevation of the farthest associated CAICS feature ("Crater_Elevation(km)", "Farthest_CAICS_Elevation(km)"), all in kilometers. Additional columns quantify the spatial

extent of ejecta and CAICS deposits ("Ejecta_Extent(km)", "CAICS_Extent(km)"), as well as crater-to-CAICS slope ("Crater-to-CAICS_Slope(%)") and ejecta and CAICS mobility indices ("Ejecta_Mobility", "CAICS_Mobility").

References

- Levy, J. S., Fassett, C. I., Head, J. W., Schwartz, C., & Watters, J. L. (2014). Sequestered glacial ice contribution to the global Martian water budget: Geometric constraints on the volume of remnant, midlatitude debris-covered glaciers. *Journal of Geophysical Research: Planets*, 119(10), 2188–2196. Retrieved 2025-02-27, from <https://onlinelibrary.wiley.com/doi/abs/10.1002/2014JE004685> (_eprint: <https://onlinelibrary.wiley.com/doi/pdf/10.1002/2014JE004685>) doi: 10.1002/2014JE004685
- Robbins, S. J., & Hynek, B. M. (2012). A new global database of Mars impact craters 1 km: 1. Database creation, properties, and parameters. *Journal of Geophysical Research: Planets*, 117(E5). Retrieved 2025-02-27, from <https://onlinelibrary.wiley.com/doi/abs/10.1029/2011JE003966> (_eprint: <https://onlinelibrary.wiley.com/doi/pdf/10.1029/2011JE003966>) doi: 10.1029/2011JE003966
- Souness, C., Hubbard, B., Milliken, R. E., & Quincey, D. (2012, January). An inventory and population-scale analysis of martian glacier-like forms. *Icarus*, 217(1), 243–255. Retrieved 2024-06-19, from <https://www.sciencedirect.com/science/article/pii/S0019103511004131> doi: 10.1016/j.icarus.2011.10.020

CAICS complex on a VFF within an impact crater (CCF (Levy et al., 2014), Crater ID 14-1-000664 (Robbins & Hynek, 2012), $39.98^{\circ}N$, $139.75^{\circ}E$). **(a)** CTX image with DEM (from CTX_064268_2183 and CTX_067922_2204). A CAICS complex lies on the debris-covered surface (boundaries highlighted by white-headed black arrows), south of a superimposed smaller crater (northern ejecta extent marked by white arrows), with topographic profile AA' from CTX DEM. **(b)** HiRISE close-up view (ESP_064268_2205) with DEM (from ESP_046374_2205 and ESP_064268_2205) and a topographic profile BB' crossing the CAICS complex. The sunlight is coming from the left in both panels. ICS=Irregular Cellular Structure, IZ=Interstitial Zone and BT=Brain coral Terrain.

Table S1. Image ID for each figures/panels.

Figure	Panel	Mission/Instrument	Image IDs	DEM Pair IDs
Fig. 1	a)	MRO/CTX	Global CTX Mosaic of Mars (V01)	
	b)	MRO/CTX	Global CTX Mosaic of Mars (V01)	
Fig. 2	a)	MRO/CTX	Global CTX Mosaic of Mars (V01)	
	b)	MRO/HiRISE	ESP_056628_2150	
	c)	MRO/HiRISE	ESP_056628_2150	
	d)	MRO/HiRISE	ESP_056628_2150	
	e)	MRO/CTX	Global CTX Mosaic of Mars (V01)	
	f)	MRO/HiRISE	ESP_048008_2215	
	g)	MRO/HiRISE	ESP_048008_2215	
	h)	MRO/HiRISE	ESP_048008_2215	
Fig. 3	a)	MRO/CTX	Global CTX Mosaic of Mars (V01)	CTX_064268_2183/ CTX_067922_2204
	b)	MRO/HiRISE	ESP_064268_2205	ESP_046374_2205/ ESP_064268_2205
Fig. S1	a)	MRO/HiRISE	ESP_056628_2150	
	b)	MRO/HiRISE	ESP_088933_2200	
	c)	MRO/HiRISE	ESP_085765_1445	
	d)	MRO/HiRISE	ESP_017264_2110	
	e)	MRO/HiRISE	ESP_025831_2260	
	f)	MRO/HiRISE	ESP_017405_2270	
Fig. S2	a)	TGO/CaSSIS	MY38_031488_354_0	
	b)	MRO/HiRISE	ESP_026584_1760	
	c)	MRO/HiRISE	ESP_026584_1760	
	d)	MRO/HiRISE	ESP_026584_1760	
Fig. S4	a)	MRO/HiRISE	ESP_088933_2200	
	b)	National Land Survey of Sweden	Swedish national LiDAR elevation data	
	c)	USGS LiDAR dataset	IA_NorthCentral_2020_D20	
Fig. S5	a)	MRO/CTX	Global CTX Mosaic of Mars (V01)	
	a')	MRO/HiRISE	ESP_056628_2150	
	b)	MRO/CTX	Global CTX Mosaic of Mars (V01)	
	b')	MRO/HiRISE	ESP_027432_2245	
	c)	MRO/CTX	Global CTX Mosaic of Mars (V01)	
	c')	MRO/HiRISE	ESP_028672_2235	
	d)	MRO/CTX	Global CTX Mosaic of Mars (V01)	
	d')	MRO/HiRISE	ESP_068561_2200	
	e)	MRO/CTX	Global CTX Mosaic of Mars (V01)	
	e')	MRO/HiRISE	ESP_028976_2245	
	f)	MRO/CTX	Global CTX Mosaic of Mars (V01)	
	f')	MRO/HiRISE	ESP_088260_2150	
	g)	MRO/CTX	Global CTX Mosaic of Mars (V01)	
	g')	MRO/HiRISE	ESP_050562_2245	
h)	MRO/CTX	Global CTX Mosaic of Mars (V01)		
h')	MRO/HiRISE	ESP_048008_221		

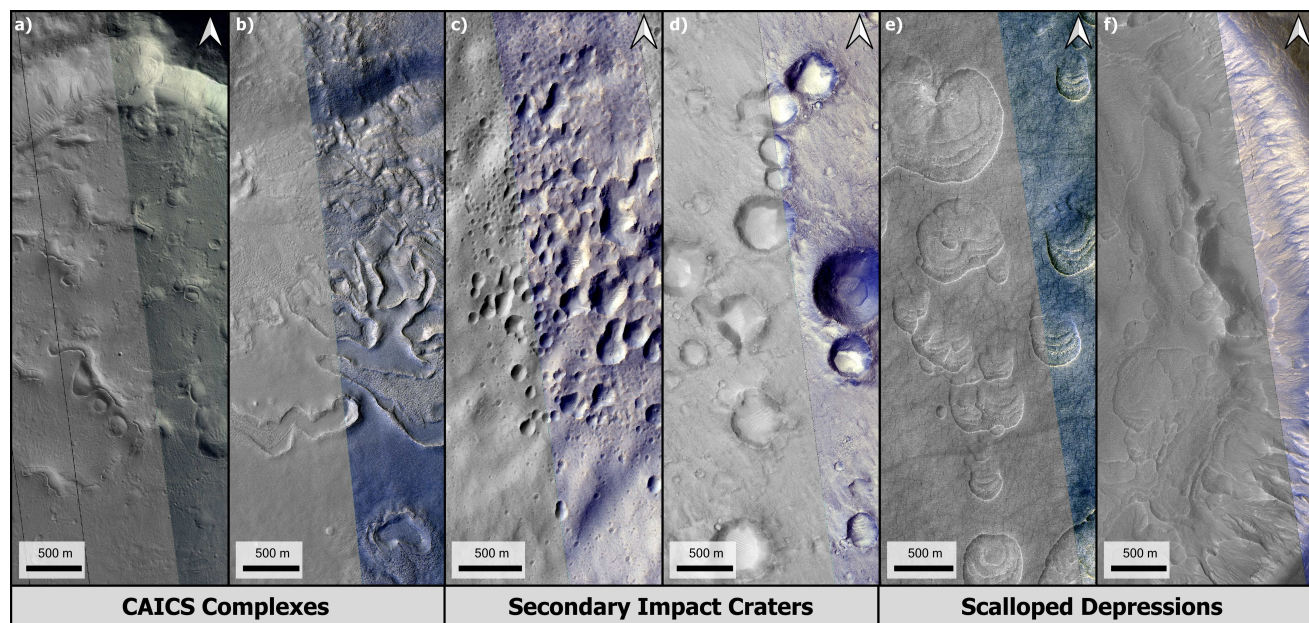


Figure S1. Morphological comparison of different clustered landforms in HiRISE images. (a-b) CAICS complexes (ESP_056628.2150 and ESP_088933.2200 respectively). (c-d) Clusters of secondary impact craters (ESP_085765.1445 and ESP_017264.2110 respectively). (e-f) Scalloped depressions (ESP_025831.2260 and ESP_017405.2270 respectively). Each panel displays an IRB color composite with the RED image in grayscale. The sunlight is coming from the top left in all panels.

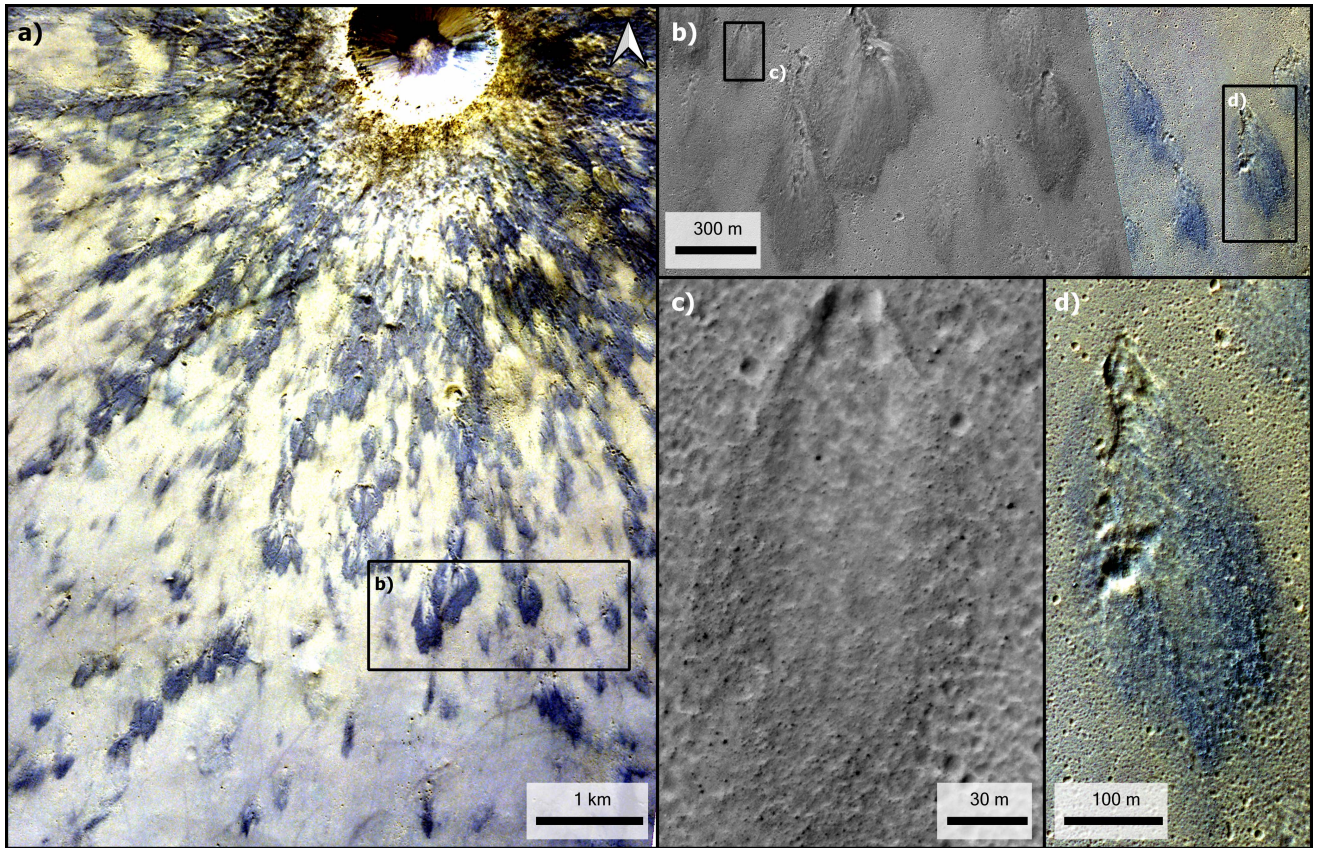


Figure S2. Images of Winslow crater ($3.73^{\circ}S$, $59.15^{\circ}E$). (a) CaSSIS image of Winslow crater in RED/PAN/BLU (MY38.031488-354.0). (b) HiRISE image of its ejecta (ESP_026584_1760 with an IRB band) with two close-up views (c) and (d). Black box marks the locations of the panel. The sunlight is coming from the top left in all panels.

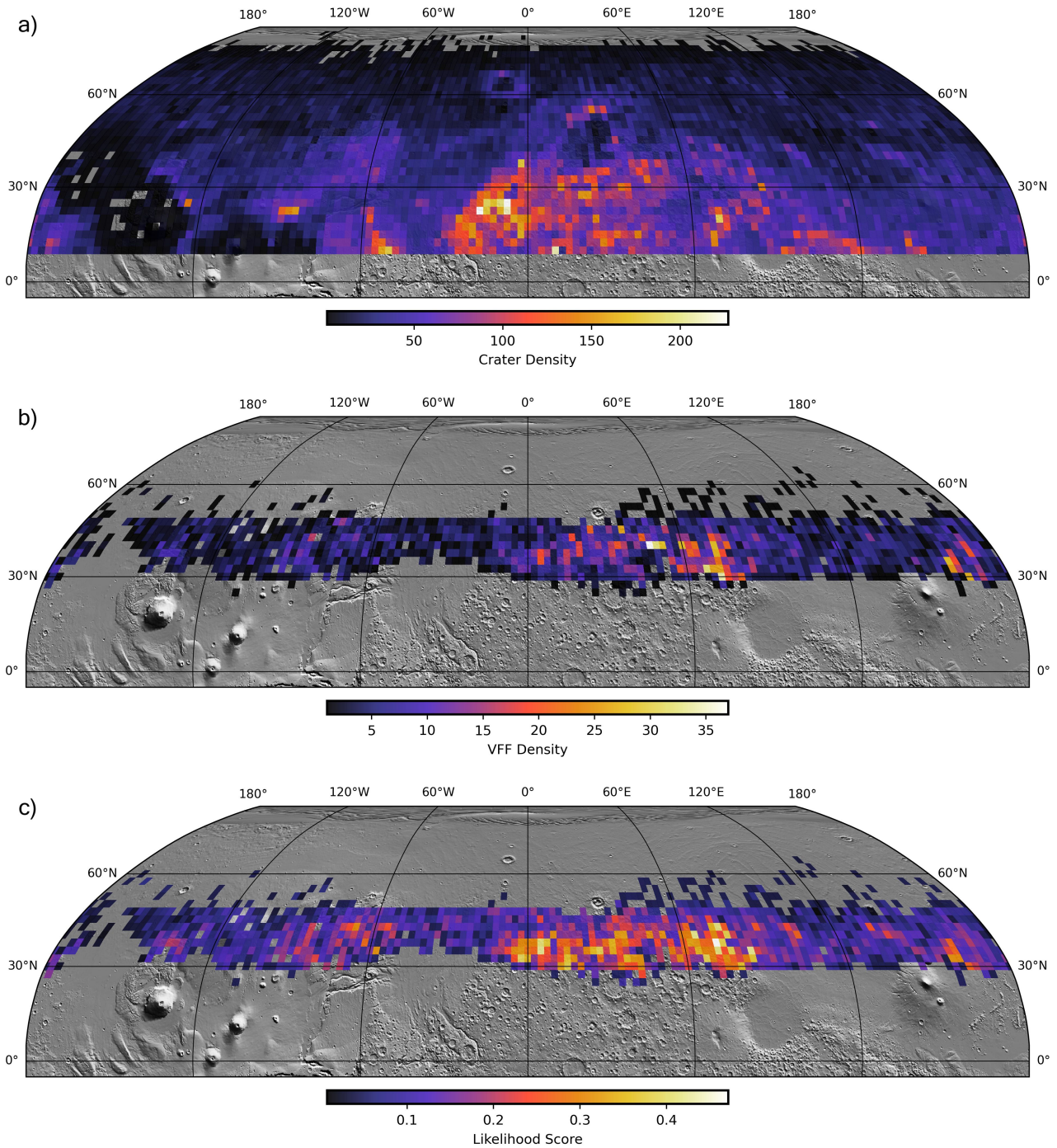


Figure S3. Density maps of the northern hemisphere ($2.5^\circ \times 2.5^\circ$ grid cells). **(a)** Density map of the crater population with a diameter ≥ 1 km from the (Robbins & Hynek, 2012) database. **(b)** Density map of the debris-covered glaciers or Viscous Flow Features (VFF), mapped by (Souness et al., 2012; Levy et al., 2014). **(c)** CAICS-likelihood map highlighting the simultaneous presence of craters and debris-covered glaciers. Global shaded MOLA image (from MOLA team, Goddard Space Flight Center, NASA) as base map with a light source from the top right.

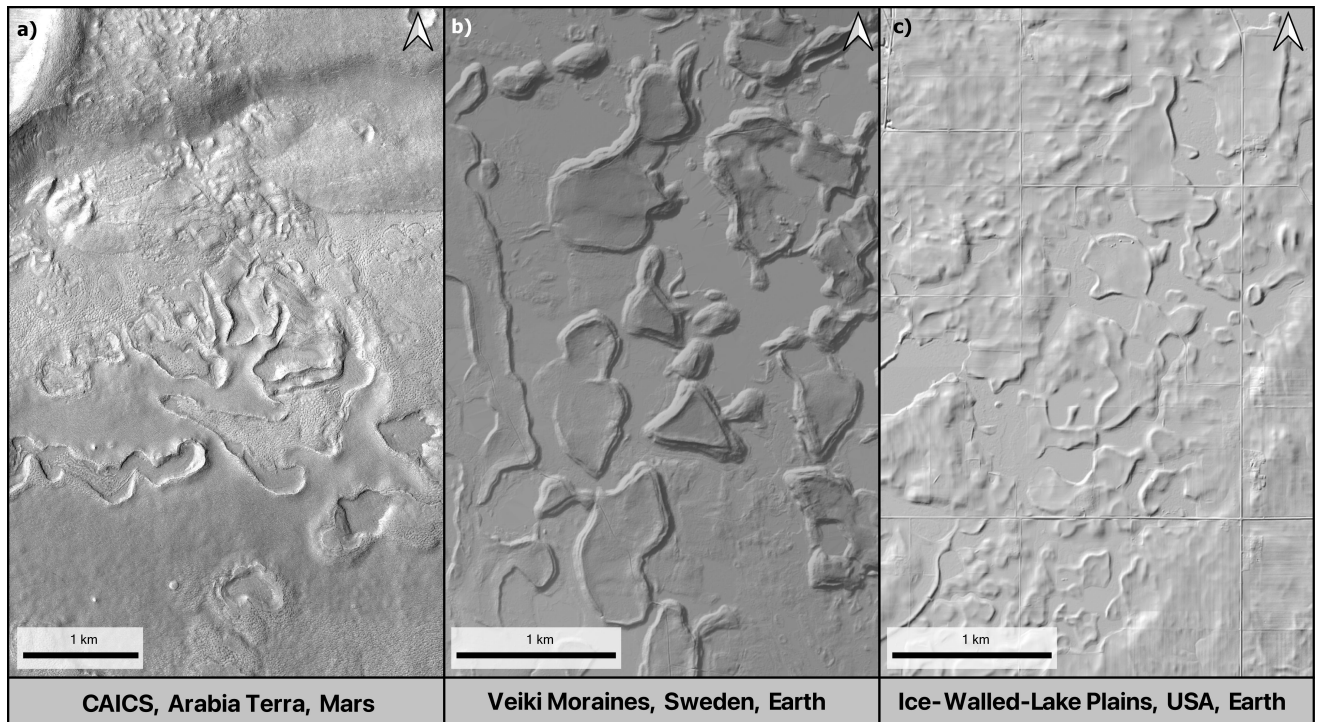


Figure S4. Morphological comparison between CAICS on Mars and terrestrial analogues, Veiki moraines and ice-walled-lake plains. (a) HiRISE image of CAICS (ESP_088933_2200). (b) Hillshade product derived from Swedish national LiDAR elevation data produced by Lantmäteriet of Veiki moraines in Sweden. View centered at $67.51^{\circ}N$, $22.61^{\circ}E$. (c) Hillshade product derived from the USGS LiDAR dataset IA_NorthCentral_2020_D20 (U.S. Geological Survey, 2020) of ice-walled-lake plains in Iowa, USA. View centered at $43.36^{\circ}N$, $-95.05^{\circ}E$. The sunlight is coming from the top left in all panels.

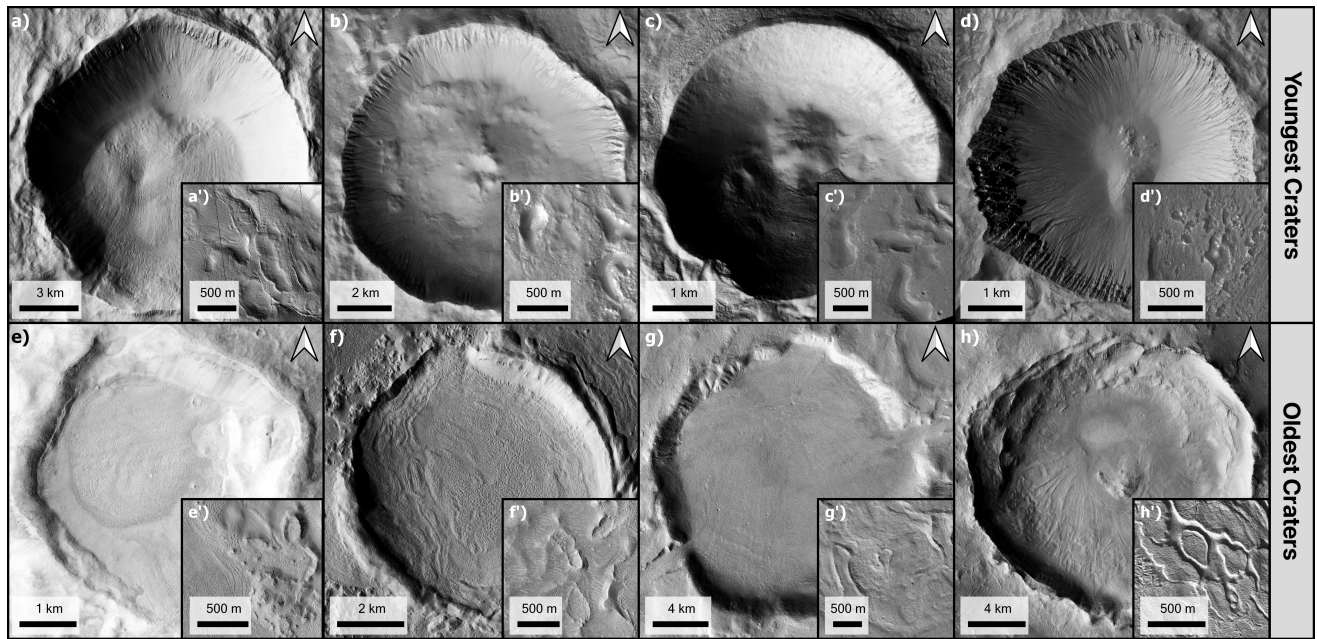


Figure S5. Examples of ones of the youngest (a-d) and the oldest (e-h) CAICS-producing impact craters from our survey, with their associated CAICS (a'-h'). (a) Crater ID 06-1-003436 (Robbins & Hynek, 2012), $34.55^{\circ}N$, $-84.61^{\circ}E$. (a') HiRISE image ESP_056628_2150. (b) Crater ID 05-1-003356 (Robbins & Hynek, 2012), $44.58^{\circ}N$, $-57.14^{\circ}E$. (b') HiRISE image ESP_027432_2245. (c) Crater ID 06-1-000369 (Robbins & Hynek, 2012), $43.06^{\circ}N$, $-65.89^{\circ}E$. (c') HiRISE image ESP_028672_2235. (d) Crater ID 06-1-001855 (Robbins & Hynek, 2012), $39.67^{\circ}N$, $-9.53^{\circ}E$. (d') HiRISE image ESP_068561_2200. (e) Crater ID 05-1-003212 (Robbins & Hynek, 2012), $38.41^{\circ}N$, $10.45^{\circ}E$. (e') HiRISE image ESP_028976_2245. (f) Crater ID 10-0-011439 (Robbins & Hynek, 2012), $34.86^{\circ}N$, $39.85^{\circ}E$. (f') HiRISE image ESP_088260_2150. (g) Crater ID 06-1-000493 (Robbins & Hynek, 2012), $43.36^{\circ}N$, $-83.73^{\circ}E$. (g') HiRISE image ESP_050562_2245. (h) Crater ID 14-1-000190 (Robbins & Hynek, 2012), $41.57^{\circ}N$, $166.71^{\circ}E$. (h') HiRISE image ESP_048008_2215. The sunlight is coming from the left in all panels.